HHS Public Access

Author manuscript

Circ Arrhythm Electrophysiol. Author manuscript; available in PMC 2018 February 01.

Published in final edited form as:

Circ Arrhythm Electrophysiol. 2017 February ; 10(2): e004434. doi:10.1161/CIRCEP.116.004434.

The Role of Apamin Sensitive Calcium Activated Small Conductance Potassium Currents on the Mechanisms of Ventricular Fibrillation in Pacing Induced Failing Rabbit Hearts

Dechun Yin, MD[1,2], **Yu-Cheng Hsieh, MD, PhD**[1,3], **Wei-Chung Tsai, MD**[1,4], **Adonis Zhi-Yang Wu, PhD**[1,5], **Zhaolei Jiang, MD**[1,6], **Yi-Hsin Chan, MD**[1,7], **Dongzhu Xu, MD, PhD**[1,8], **Na Yang, MD**[1,9], **Changyu Shen, PhD**[10], **Zhenhui Chen, PhD**[1], **Shien-Fong Lin, PhD**[1,5], **Peng-Sheng Chen, MD**[1], and **Thomas H. Everett IV, PhD**[1]

[1]Krannert Institute of Cardiology and Division of Cardiology, Department of Medicine, Indiana University School of Medicine, Indianapolis, IN

[2]Department of Cardiology, First Affiliated Hospital of Harbin Medical University, Harbin, China

[3]Cardiovascular Center, Taichung Veterans General Hospital and Department of Internal Medicine, Faculty of Medicine, Institute of Clinical Medicine, Cardiovascular Research Center, National Yang-Ming University School of Medicine, Taipei

[4]Division of Cardiology, Department of Internal Medicine, Kaohsiung Medical University Hospital, Kaohsiung University College of Medicine, Kaohsiung, Taiwan

[5]Institute of Biomedical Engineering, National Chiao-Tung University, Hsin-Chu, Taiwan

[6]Department of Cardiothoracic Surgery, Xinhua Hospital, Shanghai Jiaotong University School of Medicine, Shanghai, China

[7]Division of Cardiology, Department of Internal Medicine, Chang Gung Memorial Hospital, Chang Gung University College of Medicine, Linkou, Taoyuan, Taiwan

[8]Department of Cardiology, Faculty of Medicine, University of Tsukuba, Tsukuba, Japan

[9]Department of Gynecological and Obstetric Ultrasound, First Affiliated Hospital of Harbin Medical University, Harbin, China

[10]Richard and Susan Smith Center for Outcomes Research in Cardiology, Beth Israel Deaconess Medical Center, Harvard Medical School, Boston, MA

Abstract

Background—Ventricular fibrillation (VF) during heart failure is characterized by stable reentrant spiral waves (rotors). Apamin-sensitive small conductance calcium activated potassium currents (I_{KAS}) are heterogeneously up-regulated in failing hearts. We hypothesized that I_{KAS} influences the location and stability of rotors during VF.

Correspondence: Thomas H. Everett, IV, PhD, Division of Cardiology, Department of Medicine, Indiana University School of Medicine, 1800 N. Capitol Ave, Ste. E400E, Indianapolis, IN 46202, Tel: 317-274-0957, theveret@iu.edu.

Disclosures: None.

Methods and Results—Optical mapping was performed on 9 rabbit hearts with pacing induced heart failure. The epicardial RV and LV were simultaneously mapped in a Langendorff preparation. At baseline and after apamin (100 nmol/L) infusion, the APD_{80} was determined and VF was induced. Areas with a greater than 50% increase in the maximum APD (ΔAPD) after apamin were considered to have a high I_{KAS} distribution. At baseline, the distribution density of phase singularities (PS) during VF in high I_{KAS} distribution areas was higher than in other areas (0.0035±.0011 vs 0.0014±0.0010 PS/pixel, P=0.004). In addition, high dominant frequencies (DF) also co-localized to high I_{KAS} distribution areas (26.0 vs 17.9 Hz, P=0.003). These correlations were eliminated during VF after apamin infusion, as the number of PS (17.2 versus 11.0, P=0.009), and DFs (22.1 vs 16.2 Hz, P=0.022), were all significantly decreased. In addition, reentrant spiral waves became unstable after apamin infusion and the duration of VF decreased.

Conclusions—The I_{KAS} current influences the mechanism of VF in failing hearts as PS, high DFs, and reentrant spiral waves all correlated to areas of high I_{KAS}. Apamin eliminated this relationship and reduced VF vulnerability.

Keywords

ventricular fibrillation; heart failure; optical mapping; phase analysis; electrophysiology

Introduction

Heart failure (HF) is associated with structural and electrophysiological remodeling, that leads to tissue heterogeneities that enhances arrhythmogenesis and the propensity of sudden cardiac death.[123] Mapping studies of ventricular fibrillation (VF) have shown various mechanisms from multiple wavelets of excitation to reentrant spiral waves. The mechanisms of VF within the HF substrate have been shown to be dominated by either stable reentrant spiral waves or focal activity,[4] correlating to stable high dominant frequency (DF) areas.[5] This is in contrast to structurally normal hearts which have VF characterized by unstable reentrant spiral waves or multiple waves and transient high DF areas.[4, 5] The underlying mechanisms that support the stability of the reentrant spiral waves within the HF substrate is still unknown.

Small conductance calcium-activated potassium (SK) channels have been shown to contribute to ventricular repolarization and are mediated by calcium binding.[6] With each new study on SK channels, their importance is further demonstrated in arrhythmia vulnerability in both the atria[7] and ventricles.[8] Apamin is a specific blocker of SK currents, and apamin sensitive SK currents (I_{KAS}) have been shown to be heterogeneously upregulated within the heart failure substrate in both human studies with transplant hearts,[9, 10] and in animal models of heart failure.[11, 12] This heterogeneity has been observed both transmurally and on the same surface. Several studies have been performed investigating the role of various potassium channels (I_{KACH}, I_{Ks}, I_{Kr}, I_{K1} and I_{KATP}) have on the mechanism of VF and specifically rotor dynamics.[13] However, the role that I_{KAS} may play and whether I_{KAS} influences the location of phase singularities (PS) during VF is still unknown. The purpose of this study is to determine what role the heterogeneous I_{KAS} distribution has on the location of PS and stable reentrant spiral waves during VF in failing

hearts. We hypothesize that I_{KAS} influences the stability and location of reentrant spiral waves in the heart failure substrate.

Methods

This study protocol was approved by the Institutional Animal Care and Use Committee of Indiana University School of Medicine and the Methodist Research Institute, and conforms to the Guide for the Care and Use of Laboratory Animals. Heart failure was induction was attempted in twelve New Zealand white female rabbits via rapid ventricular pacing.[11] Among them, 9 completed the pacing protocol and developed HF. Five additional rabbits were used as controls for histology.

Pacing-Induced HF and Optical Mapping

For creation of the rabbit heart failure model, rapid ventricular pacing was performed for 3 – 5 weeks.[12] Using isoflurane for general anesthesia, a left lateral thoracotomy was performed and an epicardial pacing lead was sutured to the lateral wall of the left ventricle and connected to a modified single chamber ventricular pacemaker (Kappa or Enpulse pacemaker, Medtronic, Inc., Minneapolis, MN, USA). After recovery for 1 week, the ventricles were paced at 250 bpm for 3 days, 300 bpm for 3 days, and 350 bpm for 3-5 weeks to induce HF. Echocardiography was performed before the pacemaker was implanted and at follow up. Measurements of left ventricular diameters and fractional shortening were made from M-mode recordings of the parasternal short-axis view at the tips of the papillary muscles using the leading edge technique in three to four cardiac cycles and averaged. After the echocardiographic recordings were made, optical mapping was performed as previously described.[11] Briefly, hearts were Langendorff perfused with oxygenated Tyrode's solution (in mmol/L: NaCl 125, KCl 4.5, $NaHCO_3$ 24, NaH_2PO_4 1.8, $CaCl_2$ 1.8, $MgCl_2$ 0.5, and glucose 5.5) with a pH of 7.40. The hearts were stained with RH237 (10μmol/L) for Vm mapping. The epicardial RV and LV surfaces were illuminated at a wavelength of 532 nm, and the emitted fluorescence was filtered at 715 nm long pass.[11] Optical recordings were made from a 100×100 pixel area with a spatial resolution of 0.35×0.35 mm^2 per pixel. The signals were sampled at 2 ms/frame. Apamin, a specific SK channel blocker has been shown to heterogeneously increase the APD_{80} within the heart failure substrate, which correlates to areas of upregulated SK current.[11, 12] At baseline and after apamin (100 nmol/L) infusion, pacing was performed from the apex at 300 ms to determine APD_{80}.The cycle length was then decreased by 10 ms steps until either VF was induced or there was loss of capture. If VF was not induced, burst pacing was used for VF initiation. VF was allowed to continue for at least 3 minutes before defibrillation attempts were made. From the optical VF recordings, voltage, phase, and PS mapping was performed. In addition, an automated PS detection algorithm was applied over a 100 ms window from each VF recording as previously described.[14] The PS number was counted at five time points before a defibrillation shock was delivered, with each time point separated by 10 frames (20 ms) of data.[15] Spiral waves were defined as PS with more than one revolution period.[16] PSs associated with reentrant spiral waves were noted, and their locations were determined. The correlation of the change in APD_{80} (ΔAPD_{80}) to the location of the phase singularities was analyzed with custom LabView software. The maximum change in ΔAPD_{80} with apamin infusion was set at 100%

and no change in the APD_{80} was set at 0. The software then distributed the numbers between 0 – 100% based on their value, and colors were then assigned with blue at 0% and red at 100%. Areas with a greater than 50% change in ΔAPD_{80} after apamin infusion were considered to have a high I_{KAS} distribution. Above the 50% change in ΔAPD_{80} were the colors yellow, orange, and red. Below the 50% level were the colors green and blue. The area of the high I_{KAS} expressing regions was then calculated as a sum of the number of pixels expressing either yellow, orange or red. The area of low I_{KAS} expressing regions was calculated as the sum of the number of pixels expressing either green or blue. To further strengthen the results of the study, we also analyzed the data using 75% level change in ΔAPD_{80} after apamin infusion to define a high I_{KAS} distribution. Frequency domain analysis was also performed to quantify the VF characteristics. The highest peak within the magnitude spectrum was defined as the dominant frequency (DF).

Histology

For histology, ventricular tissue embedded in paraffin, sectioned and stained using Masson's trichrome stain. The collagen content was quantified by identifying and counting the number of blue-staining pixels as a percentage of the total tissue area using digital photomicrographs in Adobe Photoshop CS6 software.

Statistical Analysis

Data are presented as mean and 95% confidence interval (CI). Wilcoxon signed-rank test was used to compare variables measured at baseline and after apamin infusion. Mann-Whitney-Wilcoxon test was used to compare the correlation between PS density and I_{KAS} distribution as measured by ΔAPD. The P values are corrected for multiple comparison in relevant analyses using Bonferonni adjustment. The generalized estimating equations (GEEs) were used to analyze repeated measures (identify link for VF vulnerability and logit link for dichotomized VF vulnerability) with compound symmetry correlation matrix. A 2-sided P value of ≤0.05 was considered statistically significant.

Results

All rabbits that survived the rapid pacing protocol showed clinical signs of HF as previously described.[11] Table 1 shows the echocardiographic data before and after the development of heart failure. As the results in the table show, significant LV dysfunction developed with ventricular pacing.

Effects of Apamin on action potential duration (APD)

In a majority of the mapped ventricular area, apamin significantly prolonged the APD_{80} in all nine failing hearts. However, APD_{80} lengthening was not uniform across the mapped region, with some areas showing no change in APD_{80} after apamin infusion. An example of the heterogeneous APD_{80} lengthening with apamin is shown in Figure 1A with example optical signals recorded during ventricular pacing at a 300 ms cycle length (Panel B). Overall, apamin significantly increased the APD_{80} (183 [95%CI, 172–194] ms, vs 215 [95% CI, 205–224] ms, respectively, P = 0.009) within the heart failure substrate as the summary data shows in Figure 1C. The difference in APD_{80} between baseline and after apamin

infusion (ΔAPD, apamin-treated APD_{80} minus baseline APD_{80}) was used to characterize the 2-dimensional distribution of I_{KAS}. Areas with a greater than 50% change in the ΔAPD after apamin were considered to be areas with I_{KAS} upregulation.

Distribution of Phase Singularities and Spiral Waves

After VF was induced, optical mapping was used to investigate the VF mechanisms before and after infusion of apamin. Phase singularities were used to locate the sources of re-entrant VF activation[17] during a 100 ms window from each VF recording. The density of PSs in and out of the areas of I_{KAS} upregulation were calculated by measuring the distribution density of phase singularities versus the ΔAPD_{80} (Figure 2B). At baseline, PSs correlated to an increase in ΔAPD_{80}, however, this relationship disappeared after apamin infusion. An example of this correlation is demonstrated in Figure 2 (>50% ΔAPD_{80} versus <50% ΔAPD_{80}, 0.0035±.0011 vs 0.0014±0.0010 PSs/pixel, P=0.004, Fig 2C). After apamin, there was no significant correlation in the distribution of PS (>50% ΔAPD_{80} versus <50% ΔAPD_{80}, 0016±.0007 vs 0.0016±.0010 PS/pixel, P=0.791, Fig 2D). In addition, the number of PSs within the 100 ms window was significantly decreased by apamin (baseline versus apamin, 17.2 vs 11.0 PS P=0.009, Fig 2E). To strengthen the conclusions of the study, we also analyzed the data using a 75% change in ΔAPD_{80} after apamin infusion to define the areas with a high I_{KAS} distribution. As shown in Data Supplement Figure 1, there was significantly higher PS density and number of rotors in areas with a >75% change in ΔAPD_{80} as compared with the remaining portion of the mapped region.

In addition to the PS analysis, continuous reentrant spiral waves (lasting longer than 2 rotations) were identified and their location was correlated to ΔAPD_{80}. As shown in Figure 3, during VF at baseline the location of reentrant spiral waves correlated with areas of high I_{KAS} distribution. Similar to the PS, this correlation was not significant after apamin infusion.

In addition, the number of reentrant spiral waves significantly decreased after apamin (baseline versus apamin, 3.1 vs 1.3, P=0.008, Fig 3E) along with duration as they became unstable and terminated after 2.3±0.8 rotations at baseline versus 1.4±0.9 rotations after apamin (p = 0.015). Figure 4 shows the phase maps of a spiral wave before and after apamin infusion. At baseline, the reentrant spiral wave is spatially stable as the associated PS group together in a single location correlating to an area of high ΔAPD_{80}. After apamin infusion, the reentrant spiral wave meanders around the mapped region, and the associated PS does not remain spatially stable. Movies showing these VF characteristics at baseline and after apamin infusion are shown in the data supplement. The spatial stability of the reentrant spiral wave is quantified by dividing the area occupied by the spiral wave by the total area of the mapped region. The area of the spiral waves doubles with apamin (baseline vs apamin, 0.07 [Cl 0.05 – 0.09] vs 0.15 [Cl 0.07 – 0.23], p = 0.025).

Distribution of Dominant Frequencies

Frequency domain analysis was used to quantify the VF characteristics,[17] and the frequencies were then compared to the ΔAPD_{80} after apamin infusion. At baseline, the higher frequencies correlated with a greater change in the APD_{80}. This correlation was not

significant after apamin infusion as the DFs became more homogeneous. An example is shown in Figure 5 with a ΔAPD map and the corresponding static DF maps from the same heart. As the example shows, at baseline high DF areas were in similar locations as larger ΔAPD. The DFs during VF with apamin were lower and the variability did not correlate to the ΔAPD. These findings are summarized in the data shown in Figure 5 D - F

Effect of Apamin on VF Vulnerability

A total of 45 VF episodes (17 at baseline, 28 after apamin) were induced. At baseline, most of the VF episodes (15 of 17) were shock-terminated (>180 s in duration). After apamin infusion, most VF episodes (20 of 28) self-terminated (<180 s in duration) (P=0.0003). The summary data is shown in Figure 6. As the figure shows, the VF duration decreased from an average of 164 seconds (95% CI, 143–185) at baseline to 87 seconds (95% CI, 28–147) after apamin (P<0.0001).

Cardiac fibrosis

Representative trichrome sections from structurally normal and HF myocardial samples are shown in Figure 7. Compared to control, the HF myocardium contained significantly higher amount of blue-staining interstitial collagen. Quantitative collagen content measurements are also shown. The total collagen content, used as the metric of fibrosis, is nearly 4 times higher in HF than in normal myocardium (19.0 ± 1.9 versus 5.0± 1.0 % area, P =0.008).

Discussion

The main finding of this study is that significant heterogeneity of I_{KAS} is present in different regions of the epicardium in failing ventricles as indicated by the change in APD_{80} after apamin. Detailed quantitative analysis and cumulative display of PS, DFs and spiral waves showed a close co-localization to the underlying I_{KAS} distribution within the heart failure substrate. The correlation was eliminated after apamin infusion. This study further shows that the reentrant spiral waves were spatially stable at baseline, but showed meandering and wavebreak after apamin. This data indicates that I_{KAS} channels may play a role in the stability of reentrant spiral waves in the heart failure model.

Mechanisms of VF within the heart failure substrate

The structural and electrical remodeling that occur within the heart failure substrate can lead to an increase in arrhythmogenicity and ventricular fibrillation (VF) [5, 18]. Previous studies have shown that this substrate can have a significant effect on the resulting VF characteristics.[4, 5] Huang et al showed that with epicardial plaque mapping, VF in heart failure was more organized with a slower activation rate, increased incidence of block, and less reentrant wavefronts compared to structurally normal hearts.[19] Optical mapping of the epicardial surface in sheep hearts with heart failure showed a decrease in DFs and number of rotors as compared to control.[16] Recently optical mapping of the epicardial, endocardial, and transmural surfaces in a canine heart failure model showed that stable, high DF areas that correlated with spiral waves or focal activation was observed on the transmural surface at the site of the papillary muscle.[5] The control group showed significantly fewer stable, high DF areas. Non-contact mapping also showed stable reentrant rotors or focal activation in the

heart failure model, while unstable rotors characterized the VF in structurally normal hearts.[4] The current study also demonstrated that VF within the heart failure substrate was characterized by stable reentrant wavefronts. When apamin was introduced, the number of reentrant rotors decreased and when they did occur, they would not stabilize to a specific location, but would meander around the field of view.

Phase mapping is another approach that is used to further quantify VF characteristics. Phase singularities (or singularity points) are used to determine the location of wave breaks and rotor formation. It has been previously shown that VF in a heart failure model has less singularity points than control.[16] In a separate study, PSs were shown to be anatomically based in structurally normal hearts.[14] In the current study, the location of PSs were shown to correlate to areas of I_{KAS} upregulation in the heart failure substrate. Infusion of the I_{KAS} channel blocker apamin resulted in a reduced number of PS and the disappearance of an I_{KAS} correlation. These results suggest the I_{KAS} may play a role in the stabilization of rotors during VF in the heart failure model. I_{KAS} blockade by apamin shortens VF duration and promotes its spontaneous termination.[12]

SK expression in the heart failure substrate

Recent studies have shown that SK currents are upregulated in failing ventricular cardiomyocytes,[9, 11, 12, 20] along with increased SK channel protein expression and enhanced sensitivity to intracellular $Ca^{(2+)}$. Chua et al previously showed that I_{KAS} was heterogeneously upregulated in a rabbit heart failure model.[11] This heterogeneity was observed both transmurally and within the same surface. Transmural heterogeneity of I_{KAS} expression has also been shown in cardiomyocytes from heart failure transplant recipients.[9] Bonilla et al. [21] and Ni et al[20] confirmed these observations by showing that apamin significantly prolonged APD in failing human and canine ventricular cardiomyocytes, along with the increased expression of SK channel protein in failing ventricles. In the current study, the APD_{80} was heterogeneously lengthened with apamin indicating a heterogeneous upregulation of I_{KAS} and supporting the previous studies. In addition, this study shows a correlation between I_{KAS} expression and the spatial distribution of PS, DFs, and spiral waves. Stable reentrant spiral waves occurred in areas with a greater ΔAPD and were subsequently unstable and transient after apamin. This further suggests that I_{KAS} may play an important role in stabilizing reentrant spiral waves during VF within the heart failure substrate.

Ionic currents on rotor dynamics

Several studies have been performed in both animal models and computer simulation investigating the role various ionic currents have on reentrant wavefronts (ie rotors).[13] These studies have focused on rotor frequency, breakup, and stabilization versus meandering; and have shown that the potassium currents (I_{KACH}, IK_1, IK_r and IK_s) along with I_{Na} all play a role in rotor dynamics. Studies are still conflicting on the role Ca^{+2} plays. Increased intracellular Ca^{+2} has been shown to play a role in arrhythmia triggers such as DADs and EADs,[22, 23] however its influence on rotor dynamics is still unclear. Intracellular Ca^{+2} is also tied to I_{KAS} current. Recent studies have confirmed the importance of the I_{KAS} current on the repolarization reserve in failing hearts. Blocking I_{KAS} with apamin was shown to

decrease PSs and DFs during VF in a rabbit heart failure model.[12] It has previously been shown that VF within the canine heart failure substrate is characterized by stable reentrant spiral waves correlating to discrete high DF areas.[5] This study has shown that the heterogeneous upregulation of I_{KAS} plays a role in the location and stability of the PS and reentrant spiral waves. Apamin reduced the number of PS and reduced the stability of any rotors within the field of view.

Limitations

We did not measure the actual I_{KAS} current in this study with patch clamp techniques or determine the distribution of I_{KAS} channel proteins with immunohistochemistry. However, two other studies[11, 12] have documented the heterogeneous upregulation of I_{KAS} in failing ventricles. In addition, the limitations of determining the I_{KAS} protein levels in the rabbit ventricles have been discussed at length elsewhere.[12] Another limitation of the study is that the mapping was performed only on the epicardial surface. These findings may not be applicable to the midmyocardial or endocardial layers of the myocardium.

Conclusions

Ventricular fibrillation within the heart failure substrate is characterized by spatially stable rotors. Heterogeneous upregulation of I_{KAS} within this substrate provides a milieu for rotor location and stabilization. PS and DF spatial distribution, and the location of stable reentrant spiral waves correlated to greater APD changes after apamin. VF after apamin infusion eliminated this relationship as the rotors became unstable.

Supplementary Material

Refer to Web version on PubMed Central for supplementary material.

Acknowledgments

We thank Dr. Guanglong Jiang for support with the statistical analysis.

Sources of Funding: This study was supported in part by National Institutes of Health grants P01 HL78931, R01 HL71140, R41 HL124741 and R42 DA043391, a Medtronic-Zipes Endowment (Dr Chen), the Charles Fisch Cardiovascular Research Award endowed by Dr Suzanne B. Knoebel of the Krannert Institute of Cardiology, and the Indiana University Health-Indiana University School of Medicine Strategic Research Initiative.

References

1. Janse MJ. Electrophysiological changes in heart failure and their relationship to arrhythmogenesis. Cardiovasc Res. 2004; 61:208–217. [PubMed: 14736537]
2. Pogwizd SM, Bers DM. Cellular basis of triggered arrhythmias in heart failure. Trends Cardiovasc Med. 2004; 14:61–66. [PubMed: 15030791]
3. Tomaselli GF, Zipes DP. What causes sudden death in heart failure? Circ Res. 2004; 95:754–763. [PubMed: 15486322]
4. Everett, THt, Wilson, EE., Foreman, S., Olgin, JE. Mechanisms of ventricular fibrillation in canine models of congestive heart failure and ischemia assessed by in vivo noncontact mapping. Circulation. 2005; 112:1532–1541. [PubMed: 16145002]

5. Everett, THt, Hulley, GS., Lee, KW., Chang, R., Wilson, EE., Olgin, JE. The effects of remodeling with heart failure on mode of initiation of ventricular fibrillation and its spatiotemporal organization. J Interv Card Electrophysiol. 2015; 43:205–215. [PubMed: 26001644]
6. Mahida S. Expanding role of SK channels in cardiac electrophysiology. Heart Rhythm. 2014; 11:1233–1238. [PubMed: 24681007]
7. Qi XY, Diness JG, Brundel BJ, Zhou XB, Naud P, Wu CT, Huang H, Harada M, Aflaki M, Dobrev D, Grunnet M, Nattel S. Role of small-conductance calcium-activated potassium channels in atrial electrophysiology and fibrillation in the dog. Circulation. 2014; 129:430–440. [PubMed: 24190961]
8. Chan YH, Tsai WC, Ko JS, Yin D, Chang PC, Rubart M, Weiss JN, Everett THt, Lin SF, Chen PS. Small-Conductance Calcium-Activated Potassium Current Is Activated During Hypokalemia and Masks Short-Term Cardiac Memory Induced by Ventricular Pacing. Circulation. 2015; 132:1377–1386. [PubMed: 26362634]
9. Chang PC, Turker I, Lopshire JC, Masroor S, Nguyen BL, Tao W, Rubart M, Chen PS, Chen Z, Ai T. Heterogeneous upregulation of apamin-sensitive potassium currents in failing human ventricles. J Am Heart Assoc. 2013; 2:e004713. [PubMed: 23525437]
10. Yu CC, Corr C, Shen C, Shelton R, Yadava M, Rhea IB, Straka S, Fishbein MC, Chen Z, Lin SF, Lopshire JC, Chen PS. Small conductance calcium-activated potassium current is important in transmural repolarization of failing human ventricles. Circ Arrhythm Electrophysiol. 2015; 8:667–676. [PubMed: 25908692]
11. Chua SK, Chang PC, Maruyama M, Turker I, Shinohara T, Shen MJ, Chen Z, Shen C, Rubart-von der Lohe M, Lopshire JC, Ogawa M, Weiss JN, Lin SF, Ai T, Chen PS. Small-conductance calcium-activated potassium channel and recurrent ventricular fibrillation in failing rabbit ventricles. Circ Res. 2011; 108:971–979. [PubMed: 21350217]
12. Hsieh YC, Chang PC, Hsueh CH, Lee YS, Shen C, Weiss JN, Chen Z, Ai T, Lin SF, Chen PS. Apamin-sensitive potassium current modulates action potential duration restitution and arrhythmogenesis of failing rabbit ventricles. Circ Arrhythm Electrophysiol. 2013; 6:410–418. [PubMed: 23420832]
13. Pandit SV, Jalife J. Rotors and the dynamics of cardiac fibrillation. Circ Res. 2013; 112:849–862. [PubMed: 23449547]
14. Valderrabano M, Chen PS, Lin SF. Spatial distribution of phase singularities in ventricular fibrillation. Circulation. 2003; 108:354–359. [PubMed: 12835210]
15. Hayashi H, Lin SF, Chen PS. Preshock phase singularity and the outcome of ventricular defibrillation. Heart Rhythm. 2007; 4:927–934. [PubMed: 17599680]
16. Moreno J, Zaitsev AV, Warren M, Berenfeld O, Kalifa J, Lucca E, Mironov S, Guha P, Jalife J. Effect of remodelling, stretch and ischaemia on ventricular fibrillation frequency and dynamics in a heart failure model. Cardiovasc Res. 2005; 65:158–166. [PubMed: 15621043]
17. Clayton RH, Holden AV. A method to quantify the dynamics and complexity of re-entry in computational models of ventricular fibrillation. Phys Med Biol. 2002; 47:225–238. [PubMed: 11837614]
18. Holzem KM, Efimov IR. Arrhythmogenic remodelling of activation and repolarization in the failing human heart. Europace. 2012; 14:v50–v57. doi: 10.1093/europace/eus1275. [PubMed: 23104915]
19. Huang J, Rogers JM, Killingsworth CR, Walcott GP, KenKnight BH, Smith WM, Ideker RE. Improvement of defibrillation efficacy and quantification of activation patterns during ventricular fibrillation in a canine heart failure model. Circulation. 2001; 103:1473–1478. [PubMed: 11245655]
20. Ni Y, Wang T, Zhuo X, Song B, Zhang J, Wei F, Bai H, Wang X, Yang D, Gao L, Ma A. Bisoprolol reversed small conductance calcium-activated potassium channel (SK) remodeling in a volume-overload rat model. Mol Cell Biochem. 2013; 384:95–103. [PubMed: 23975505]
21. Bonilla IM, Long VP 3rd, Vargas-Pinto P, Wright P, Belevych A, Lou Q, Mowrey K, Yoo J, Binkley PF, Fedorov VV, Gyorke S, Janssen PM, Kilic A, Mohler PJ, Carnes CA. Calcium-activated potassium current modulates ventricular repolarization in chronic heart failure. PLoS One. 2014; 9:e108824. [PubMed: 25271970]

22. Zhao Z, Wen H, Fefelova N, Allen C, Baba A, Matsuda T, Xie LH. Revisiting the ionic mechanisms of early afterdepolarizations in cardiomyocytes: predominant by Ca waves or Ca currents? Am J Physiol Heart Circ Physiol. 2012; 302:H1636–1644. [PubMed: 22307670]

23. Ter Keurs HE, Boyden PA. Calcium and arrhythmogenesis. Physiol Rev. 2007; 87:457–506. [PubMed: 17429038]

WHAT IS KNOWN

- Ventricular fibrillation during heart failure is characterized by stable reentrant spiral waves (rotors).
- Apamin-sensitive small conductance calcium activated potassium currents (I_{KAS}) are heterogeneously up-regulated in failing hearts.

WHAT THE STUDY ADDS

- The I_{KAS} current influences the mechanism of ventricular fibrillation in failing hearts.
- Heterogeneous upregulation of I_{KAS} within this substrate provides a milieu for rotor location and stabilization.
- The spatial distribution phase singularities and dominant frequencies, and the location of stable reentrant spiral waves correlated to greater action potential duration changes after apamin infusion.
- Ventricular fibrillation after apamin infusion eliminated this relationship as the rotors became unstable.

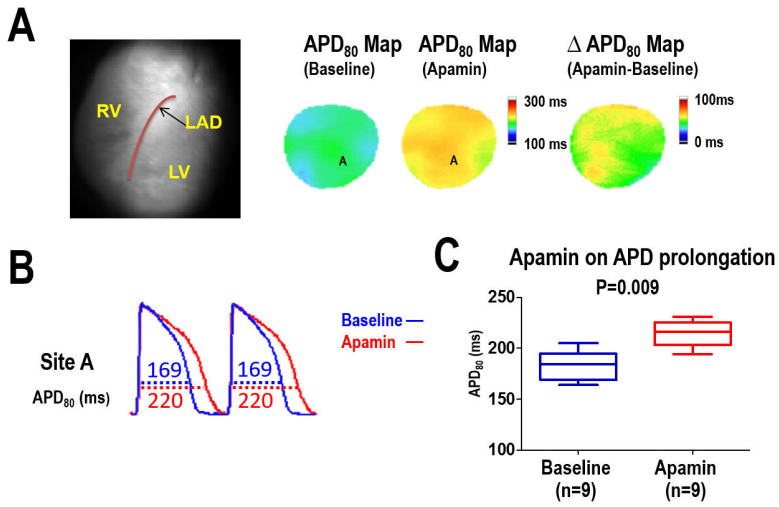

Figure 1.

Effect of apamin on APD_{80} prolongation in HF ventricles. **A**, APD_{80} map before and after apamin infusion in a failing heart. The ΔAPD_{80} map shows a heterogeneous distribution of APD prolongation with apamin. **B**, APD_{80} trace before (blue line) and after (red line) apamin infusion at pacing cycle length (PCL) 300ms. **C,** Summary data shows that the APD_{80} and was significantly prolonged after apamin infusion in HF ventricles.

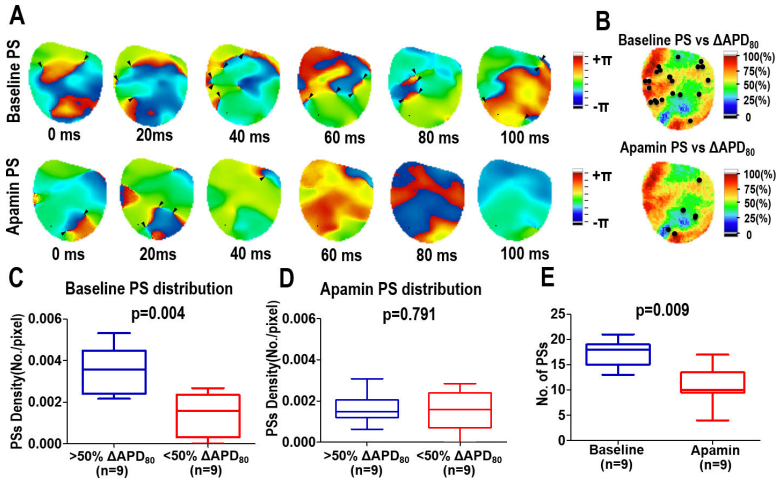

Figure 2.

Effects of apamin on phase singularities during VF in heart failure. **(A)** Consecutive phase maps sampled at 20 ms intervals during VF at baseline (top) and after apamin (bottom). Phase singularities are indicated by black arrowheads. **(B)** Correlation of spiral waves (rotor) to ΔAPD. Summary data showing the correlation of the density of PS at baseline **(C)** and after apamin **(D)** to ΔAPD. **(E)** Summary data showing the overall effect of apamin on the number of PS.

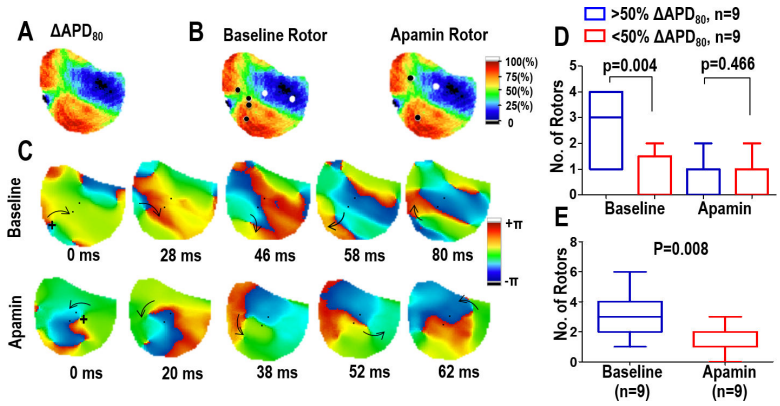

Figure 3.

Spatial distribution of reentrant spiral waves (rotors). Panels **(A)** and **(B)** Correlation of the location of rotors to ΔAPD_{80}. At baseline, most of the rotors occur in high I_{KAS} areas. This correlation is not seen with apamin. **(C)** Consecutive phase maps sampled at 20 ms intervals during VF at baseline (top) and after apamin (bottom). Arrows indicate the direction of rotation. The rotor observed at baseline remains spatially stable while the rotor with apamin meanders around the field of view. **(D)** Summary data showing the correlation of the location of rotors to ΔAPD. **(E)** Summary data showing the overall effect of apamin on the number of rotors.

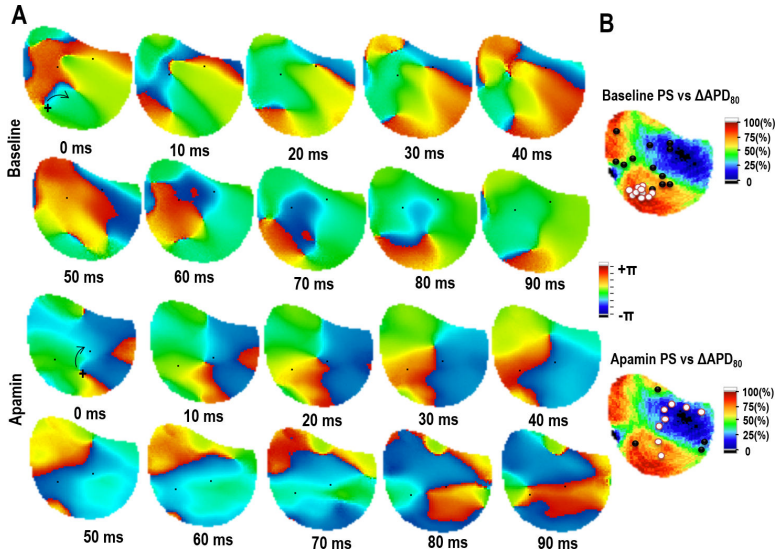

Figure 4.

Tracking the location of phase singularities from a reentrant spiral wave. **(A)** PS associated with a reentrant spiral wave at baseline (top panels) and after apamin (bottom panels). The PS is tracked for 90 ms showing the stability of the PS. **(B)** Summary data showing the location of the PS during the reentrant spiral wave correlated to the change in APD_{80} with apamin. White dots indicate the PS associated with the spiral wave. Black dots indicate PS associated with wave break.

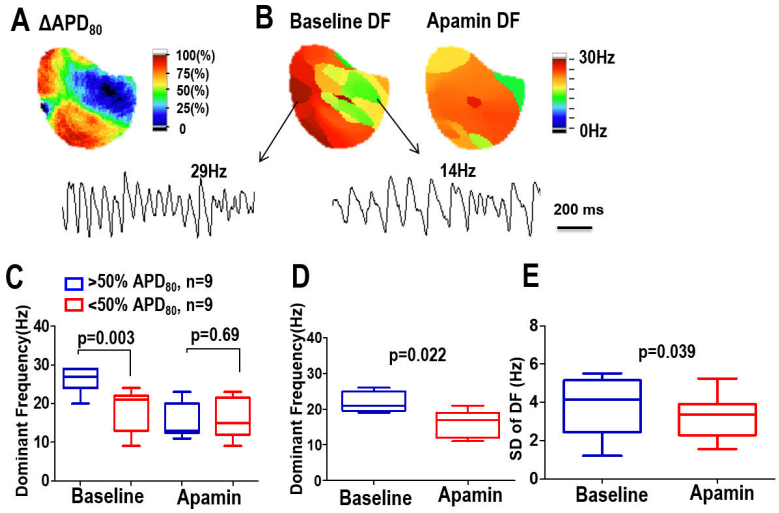

Figure 5.

ΔAPD_{80} and DF. **(A)** In a heart failure rabbit model, the change in APD_{80} after apamin infusion (apamin-treated APD_{80} minus baseline). **(B)** Static DF maps during VF before and after apamin injection. High DF areas correlated with areas of high I_{KAS} current distribution. This correlation was eliminated with apamin. Summary data for all hearts is shown in panel **(C)**. **(D)** Summary data of the DFs before and after apamin. **(E)** Summary data of the heterogeneity of the DFs before and after apamin.

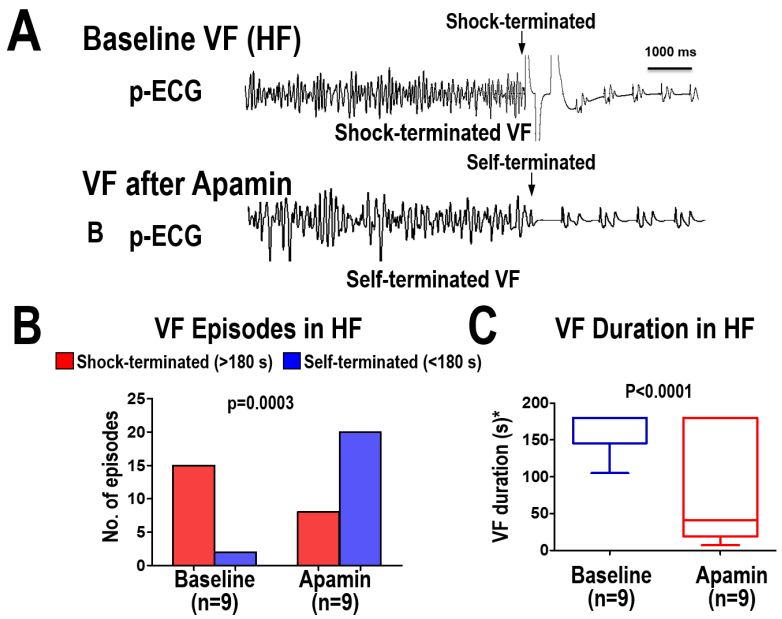

Figure 6.

VF vulnerability after I_{KAS} blockade in the heart failure substrate. (A) ECG recording during VF at baseline (shock terminated) and after apamin infusion (self-terminated). Sustained VF was defined as lasting at least 180 seconds before a shock was delivered. Summary data in Panels B and C show that apamin increased the number of VF episodes that self-terminated which corresponded to a shorter VF duration.

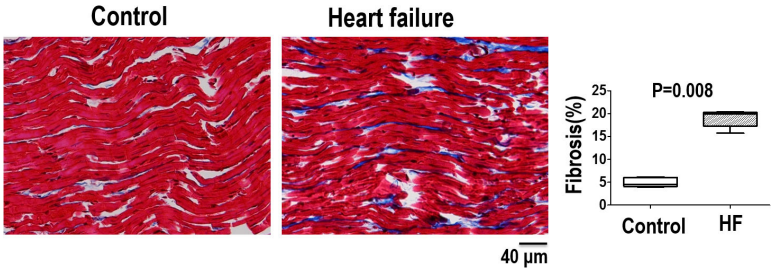

Figure 7.

Amount and distribution of fibrosis from Masson's trichrome staining of ventricular tissue samples from structurally normal hearts (control) and heart failure hearts. Summary data shows the heart failure group had a significantly larger amount of fibrosis compared to the control group.

Table 1

Echocardiographic Studies

	Before Pacing	After Pacing	P value
LVEDD (mm)	12.0±1.6	17.2±1.1	< 0.001
LVESD (mm)	7.6±1.3	15.1±1.0	< 0.001
FS(%)	36.8±6.1	12.2±6.9	< 0.001
EF(%)	70.3±7.9	28.4±5.9	< 0.001

Values are means ± SD. LVEDD – left ventricular end diastolic diameter; LVESD – left ventricular end systolic diameter; FS – fractional shortening; EF – ejection fraction